Carrier dynamics in low-temperature grown GaAs studied by terahertz emission spectroscopy

H. Němec, A. Pashkin, and P. Kužel[a)]
Institute of Physics, Academy of Sciences of the Czech Republic, and Center for Molecular Systems and Biomolecules, Na Slovance 2, 182 21 Prague 8, Czech Republic

M. Khazan, S. Schnüll, and I. Wilke
Institut für Angewandte Physik, Universität Hamburg, Jungiusstrasse 11, D-20355 Hamburg, Germany

(Received 16 January 2001; accepted for publication 25 April 2001)

Ultrafast dynamics of free carriers in low-temperature grown GaAs was studied using time-domain terahertz emission spectroscopy. The subpicosecond free-carrier lifetime was determined for a set of annealed samples with different growth temperatures (175–250 °C), the carrier mobility was also estimated. The influence of the growth temperature on the ultrafast carrier trapping is discussed.
© *2001 American Institute of Physics.* [DOI: 10.1063/1.1380414]

I. INTRODUCTION

Low-temperature grown GaAs is the most widely used material for the fabrication of photoconductive THz emitters or detectors. Its unique properties are good carrier mobility, high dark resistivity, and subpicosecond carrier lifetimes.

GaAs grown by molecular beam epitaxy (MBE) at temperatures lower than 300 °C (LT GaAs) presents a 1%–2% arsenic excess which depends on the growth temperature T_g and on the arsenic pressure during the deposition.[1,2] As a result a high density of arsenic antisite defects As_{Ga} is produced and forms a donor miniband close to the center of the band gap.[3,4] The concentration of As_{Ga} increases with decreasing T_g and can reach $10^{19}-10^{20}\,cm^{-3}$, which leads to a decrease of the resistivity due to hopping conduction.[5–7] The concentration of ionized donors As_{Ga}^{+}, which are responsible for the fast electron trapping, depends strongly on the concentration of acceptors (gallium vacancies).[8] The as-grown samples are then usually thermally annealed: The excess arsenic precipitates into metallic clusters surrounded by depleted regions of As/GaAs barriers which allow one to recover the high resistivity.[9] The role of the precipitates in the fast carrier recombination process is, however, not yet completely clear. Recently, attempts have been made also to dope LT GaAs during the MBE growth with compensating acceptors, namely with Be, in order to increase the number of As_{Ga}^{+}: the trapping time reduction was observed for heavily doped samples.[10,11]

A detailed understanding of the mechanisms of the ultrafast response is a crucial point that allows one to optimize the elaboration technology and to control the properties of the material. As the photocarrier trapping is a nonradiative process in undoped LT GaAs samples, photoluminescence measurements cannot be used for the carrier lifetime determination.[3,11] The most commonly applied technique is thus the optical pump–probe experiment.[3,10,12–17] However, the interpretation of the obtained pump–probe signals is difficult as (i) several decay components are usually observed including the photocarrier trapping and cooling, and the photoinduced absorption,[18] and as (ii) high excited-carrier densities ($10^{17}-10^{19}\,cm^{-3}$) have to be used. Consequently, a large number of physical phenomena can contribute to the observed signal: band filling, carrier scattering, band-gap renormalization, free-carrier absorption, trapped-carrier reabsorption, filling of the miniband states. The observed effects thus depend significantly on the pump intensity and on the pump/probe wavelength. These problems can be avoided using the optical pump–terahertz (THz) probe experiments as discussed in Ref. 19; on the other hand, the temporal resolution in these experiments is decreased to about 400 fs due to the length of the THz pulses.

In this contribution we propose a method for extracting the subpicosecond photoexcited carrier dynamics directly from the temporal wave form of the THz pulses which are emitted from a biased LT GaAs sample. The advantage of this method is that the photo-induced absorption is avoided, that the measurement is not sensitive to the carrier cooling, and that low carrier densities (less than $10^{15}\,cm^{-3}$) are used: Thus the trap filling and the screening of the carriers can be completely neglected. Also, time constants as small as 250 fs can be detected.

II. EXPERIMENTAL METHOD AND RESULTS

The samples investigated in this study were grown by MBE on a semi-insulating GaAs substrate: First, a 72.5 nm GaAs buffer layer was deposited at 600 °C, subsequently, a 1.3 μm layer was grown at a temperature T_g. Four samples were prepared with $T_g = 175$, 200, 225, and 250 °C. The samples were then annealed for 10 min at 600 °C. Gold planar electrodes were deposited on the layer surface with two different spacings (4 and 6 mm).

During the experiments a high bias voltage was applied on the electrodes (between 800 and 2500 V), the space between them was then uniformly irradiated by a femtosecond pulse train coming from a Ti:sapphire oscillator ($\lambda = 800\,nm$, $t_p = 100\,fs$, repetition rate 76 MHz): the generated free-electron densities ranged from 10^{14} to $10^{15}\,cm^{-3}$. The

[a)]Electronic mail: kuzelp@fzu.cz

 © 2001 American Institute of Physics

Downloaded 24 Oct 2001 to 195.113.33.31. Redistribution subject to AIP license or copyright, see http://ojps.aip.org/japo/japcr.jsp

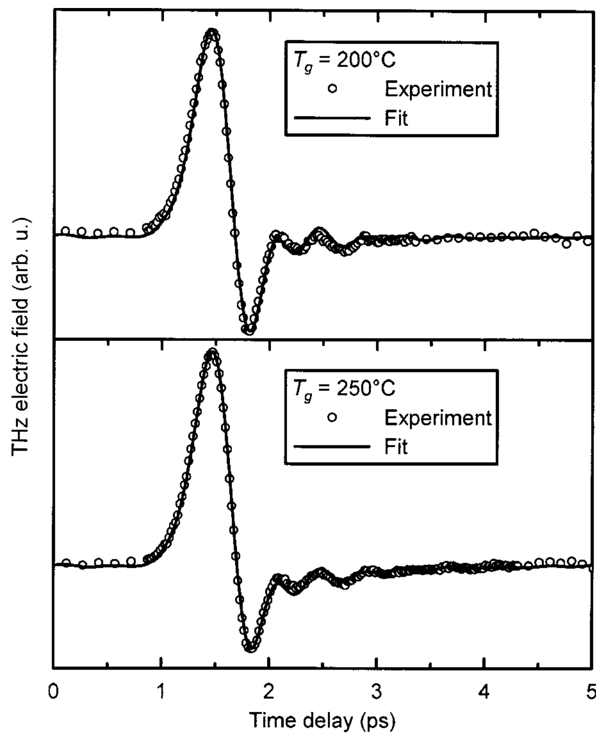

FIG. 1. Examples of the THz wave form in the far field for different growth temperatures.

emitted THz signal was detected in the far field through electro-optic (EO) sampling using a 1-mm-thick ⟨110⟩ ZnTe crystal.[20] The far-field profile of the THz pulse is proportional to the time derivative of the current between the electrodes.[21,22] It is important to stress that no focusing optics should be used in the path of the THz beam in order to avoid the wave form distortion due to the phase change and spectral filtering.[22] In our approach the whole shape of the THz electric field is fitted in contrast with the emission experiments carried out in quantum wells and superlattices[23,24] where only the resonant frequency was being determined, and that are thus less sensitive to the presence of mirrors and lenses.

The experiments were performed under nitrogen atmosphere in order to avoid water vapor absorption. We verified for all studied samples that, within the above-specified ranges, the shape of the THz wave forms depends neither on the distance between the electrodes, nor on the magnitude of the applied voltage, nor on the incident light intensity. Examples of the measured wave forms are given in Fig. 1. The shape of the wave forms is essentially given by the dynamics of the carriers in the LT GaAs layer and in the GaAs substrate (13% of the incident power is absorbed in the bulk) and by the detection process in the ZnTe sensor.

The relation between the true THz wave form and the wave form obtained through the EO sampling has already been described:[25,26] The complex THz spectrum is simply multiplied by the autocorrelation of the optical pulse and by spectral characteristics of the EO crystal [see Eq. (61) in Ref. 26]. We have experimentally determined the THz dielectric spectrum and the group refractive index near 800 nm for our ZnTe sensor. These data were then used for the fitting.

III. THEORETICAL MODEL AND DISCUSSION

The transient current density j through the emitter causes the emission of a THz field E_{THz}. Far from the emitter, the on-axis field is given by

$$E_{\mathrm{THz}} \propto \int \frac{\partial j}{\partial t} dx\, dy\, dz, \tag{1}$$

where the integration is taken over the whole emitter. The current density depends on the free-carrier concentration n and on the mean velocity v of the electrons:

$$j = -env, \tag{2}$$

the contribution of the holes which have a much smaller mobility is neglected. Our model of the carrier transport is based on a set of kinetic equations[27] which can be written for the LT GaAs layer as well as for the GaAs substrate as follows:

$$\frac{dn}{dt} = -\frac{n}{\tau_c} + G(t,\mathbf{r}), \tag{3}$$

$$\frac{dv}{dt} = -\frac{v}{\tau_s} + \frac{eE_{\mathrm{loc}}(\mathbf{r})}{m^*} - \frac{vG(t,\mathbf{r})}{n}, \tag{4}$$

where G is a photoinjection rate, E_{loc} is the local electric field, τ_c is the free-electron lifetime, and τ_s is the velocity relaxation time. A term describing the carrier diffusion was omitted in Eq. (3) as it has no impact on the subpicosecond dynamics. The last term of Eq. (4) allows one to define correctly the mean velocity v of the free carriers during the generation process: $dn = G\, dt$ is the density of the newly generated carriers with zero average speed, thus the change of the average speed of all the carriers is

$$dv = -v \frac{G(t,\mathbf{r})dt}{n}. \tag{5}$$

This treatment is necessary as the velocity relaxation time in the substrate is longer than the excitation optical pulse.

If the emitter is irradiated at normal incidence, the photoinjection rate G can be factorized:

$$G(t,\mathbf{r}) = g(t)h(x,y)f(z), \tag{6}$$

where the z axis is normal to the emitter surface. We used an excitation beam with a diameter exceeding the gap between the electrodes, consequently $h(x,y)$ is only a very slowly varying function. As Eq. (3) is linear with constant coefficients, and since the initial carrier concentration is negligible, the free-carrier concentration can be factorized in a very similar form:

$$n(t,\mathbf{r}) = n(t)h(x,y)f(z). \tag{7}$$

We assume that the variation of the local electric field E_{loc} along z is very slow near the surface where most of the carriers are generated. Using similar arguments as for the free-carrier concentration, the solution of Eq. (4) can be written in the form:

$$v(t,\mathbf{r}) = v(t)E_{\mathrm{loc}}(x,y). \tag{8}$$

It can be then shown that Eq. (1) becomes after the integration:

Downloaded 24 Oct 2001 to 195.113.33.31. Redistribution subject to AIP license or copyright, see http://ojps.aip.org/japo/japcr.jsp

TABLE I. Free-electron lifetime and mobility in LT GaAs for different growth temperatures.

T_g(°C)	$\tau_c^{\mathrm{LT}}(fs)$	μ (cm^2 V^{-1} s^{-1})
250	660±50	2250±100
225	450±50	2350±100
200	375±50	3000±500
175	280±100	⋯

$$E_{\mathrm{THz}} \propto \frac{\partial}{\partial t}(\alpha^{\mathrm{LT}} n^{\mathrm{LT}}(t) v^{\mathrm{LT}}(t) + \alpha^B n^B(t) v^B(t)), \tag{9}$$

where the superscripts LT and B stand for the layer and the substrate, respectively; α is the fraction of the absorbed power (82% for the layer, and 18% for the substrate). The bulk lifetime τ_c^B is significantly longer than τ_c^{LT} and therefore it cannot contribute to the measured fast dynamics. The mobility of the free carriers in the bulk, which is connected to τ_s^B, is supposed to be known (7000 cm^2 V^{-1} s^{-1}).[28] Our model is thus fully determined by three fitting parameters: τ_c^{LT}, τ_s^{LT}, and a proportionality constant.

The results of the fits are given in Table I. The lifetimes are also plotted in Fig. 2, along with the data obtained by an optical pump–THz probe experiment which provides access to the same parameters under similar experimental conditions. Our values of the electron mobility have the same order of magnitude as those reported in Refs. 19 and 29. For the samples grown at 225 and 250 °C the mobilities agree within the error margins. The slightly higher mobility of the sample grown at 200 °C is not considered to be significant. It is attributed to a lower precision in the determination of τ_s^{LT} for the samples with faster dynamics.

The time constants τ_c^{LT} and τ_s^{LT} are the principal results of the time-domain terahertz emission spectroscopy (TDTES) measurements. Next, we will briefly discuss the physical meaning associated with these time constants.

The lifetime τ_c^{LT} corresponds to the electron trapping time as long as the number of photoexcited carriers is significantly lower than the number of traps. This condition is very well fulfilled in our experiment. The number of traps is determined by the excess arsenic incorporated in the material during MBE growth. For LT GaAs samples grown at temperatures between 200 and 250 °C the concentration of excess arsenic N_{T_g} ranges from 6.6 to 1.3×10^{19} cm^{-3} (Ref. 9) and is therefore four to five orders of magnitude larger than the photocarrier density $n = 10^{14}$–10^{15} cm^{-3}. Although a quantitative model of precipitate formation during the post-growth annealing has not yet been developed, we are convinced that the remaining antisite defect density is significantly larger than the excitation density in the TDTES measurements. This is supported by the observation that the measured temporal shape of the THz transients is independent of incident laser intensity.

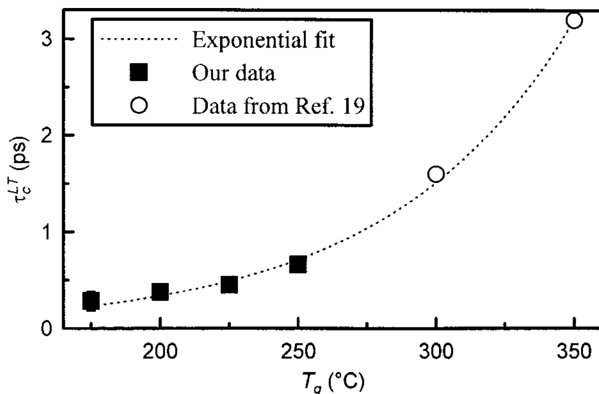

FIG. 2. Free-electron lifetimes in LT GaAs.

The momentum scattering time τ_s^{LT} determines the mobility of the free electrons. The phonon scattering is the dominant scattering mechanism at room temperature in single crystals of GaAs. In contrast, for heavily damaged materials like LT GaAs elastic scattering by neutral and ionized impurities prevails.[30] The mobilities of our samples are 2250–3000 cm^2 V^{-1} s^{-1}. These values are in good agreement with theory of neutral impurity scattering in GaAs with a neutral impurity density of $N_{\mathrm{ni}} = (4.1-5.4)\times 10^{18}$ cm^{-3} [Ref. 31].

The velocity that the photocarriers acquire due to the applied bias field in our experiments does not exceed the thermal velocity. Therefore, the scattering cross section which follows the $1/v^4$ law for elastic scattering[32] is not influenced by the bias voltage. This again agrees with the observation that the temporal shape of the THz transient is independent of the applied bias voltage.

In our experiment the excitation wavelength is $\lambda = 800$ nm: The photoexcited carriers acquire an excess energy of 130 meV. In case of low photoexcitation densities the trapping times are also independent of the excitation wavelength as has been demonstrated recently.[19]

The free-electron lifetimes we obtained agree very well with the values reported in Ref. 19 for samples grown at slightly higher temperatures. The whole set of lifetimes can be fitted by an exponential function

$$\tau_c^{\mathrm{LT}} = \tau_0 \exp(T_g/T_0) \tag{10}$$

with $T_0 = 66$ °C, and $\tau_0 \approx 20$ fs. We can write the free-electron lifetime as[3]

$$\tau_c^{\mathrm{LT}} = 1/(N v_t \sigma) = 1/(\pi N R^2 s v_t), \tag{11}$$

where N is the defect density, R is the average defect radius, σ is the capture cross section, s describes the ability of the defect to capture an electron, and v_t is the electron velocity which is in our case practically equal to the thermal velocity. Within the unified As cluster model[9] the amount of the elemental arsenic is given by the sample growth temperature and remains constant during subsequent annealing. This can be expressed by

$$N_g R_g^3 = N_A R_A^3, \tag{12}$$

where the index g stands for an as-grown sample and A stands for an annealed sample. Putting together Eqs. (11) and (12), and assuming, as shown in Ref. 9, that:

$$N_g = N_{g_0} \exp(-T_g/T_{g_0}), \tag{13a}$$

$$N_A = N_{A_0} \exp(-T_A/T_{A_0}) \tag{13b}$$

Downloaded 24 Oct 2001 to 195.113.33.31. Redistribution subject to AIP license or copyright, see http://ojps.aip.org/japo/japcr.jsp

one obtains:

$$\tau_c^{\mathrm{LT}}(T_g, T_A) = \tau_0 \exp(2T_g/(3T_{g_0})), \tag{14}$$

with

$$\tau_0 = \frac{\exp(T_A/(3T_{A_0}))}{\pi R_g^2 v_t s (N_{A_0} N_{g_0}^2)^{1/3}}. \tag{15}$$

Using values given in Ref. 9, the value of τ_0 can be estimated: one finds $\tau_0 \approx 25$ fs for $s=1$ and $R_g \approx 2.3$ Å, which is very close to the result of our fit. On the other hand, our fit yields $T_{g_0} = 44\,°\mathrm{C}$. This value is slightly larger than the value reported in Ref. 9 ($T_{g_0} = 30\,°\mathrm{C}$) which was obtained from measurements of as-grown samples (let us recall that our samples were annealed at 600 °C). From this difference, we conclude that the annealing slows down the dynamics of LT GaAs grown at lower temperatures stronger than the dynamics of samples grown at higher temperatures. This suggests, in turn, that the ability of electron capture is reduced for As clusters comparing to point defects.

IV. CONCLUSION

In conclusion, we demonstrated the method of extraction of the ultrashort carrier lifetime directly from the terahertz wave forms emitted by biased samples. We determined the electron lifetimes and mobilities for several annealed LT GaAs samples grown at different temperatures. A simple geometrical model was used to relate these results to the previously published ones.

ACKNOWLEDGMENTS

Fruitful discussions with T. Korn and support through LT GaAs MBE-growth by W. Hansen and C. Heyn are acknowledged. This work was supported by the Ministry of Education of the Czech Republic (Project No. LN00A032).

[1] M. Kaminska, Z. L. Eber, E. R. Weber, and T. George, Appl. Phys. Lett. **4**, 1881 (1989).
[2] R. P. Mirin, J. P. Ibbetson, U. K. Mishra, and A. C. Gossard, Appl. Phys. Lett. **65**, 2335 (1994).
[3] S. Gupta, J. F. Whitaker, and G. A. Mourou, IEEE J. Quantum Electron. **28**, 2464 (1992).
[4] D. C. Look, D. C. Walters, M. O. Mansreh, J. R. Sizelove, C. E. Stutz, and K. R. Evans, Phys. Rev. B **42**, 3578 (1990).
[5] X. Liu, A. Prasad, W. M. Chen, A. Kurpiewski, A. Stoschek, Z. Liliental-Weber, and E. R. Weber, Appl. Phys. Lett. **65**, 3002 (1994).
[6] H. Yamamoto, Z. Q. Fang, and D. C. Look, Appl. Phys. Lett. **57**, 1537 (1990).
[7] K. Khirouni, M. Stellmacher, J. Nagle, and J. C. Bourgoin, Solid-State Electron. **43**, 589 (1999).
[8] M. Stellmacher, J.-P. Schnell, D. Adam, and J. Nagle, Appl. Phys. Lett. **74**, 1239 (1999).
[9] J. K. Luo, H. Thomas, D. V. Morgan, and D. Westwood, J. Appl. Phys. **79**, 3622 (1996).
[10] M. Haiml, U. Siegner, F. Morier-Genoud, U. Keller, M. Luysberg, P. Specht, and E. R. Weber, Appl. Phys. Lett. **74**, 1269 (1999).
[11] A. Krotkus, K. Bertulis, L. Dapkus, U. Olin, and S. Marcinkevičius, Appl. Phys. Lett. **75**, 3336 (1999).
[12] A. J. Lochtefeld, M. R. Melloch, J. C. P. Chang, and E. S. Harmon, Appl. Phys. Lett. **69**, 1465 (1996).
[13] U. Siegner, R. Fluck, G. Zhang, and U. Keller, Appl. Phys. Lett. **69**, 2566 (1996).
[14] P. W. E. Smith, S. D. Benjamin, and H. S. Loka, Appl. Phys. Lett. **71**, 1156 (1997).
[15] H. S. Loka, S. D. Benjamin, and P. W. E. Smith, Opt. Commun. **161**, 232 (1999).
[16] S.-F. Horng, S.-H. Lu, J.-S. Yu, T.-R. Tsai, and C.-C. Chi, Opt. Quantum Electron. **32**, 573 (2000).
[17] J.-F. Roux, J.-L. Coutaz, and A. Krotkus, Appl. Phys. Lett. **74**, 2462 (1999).
[18] S. H. Benjamin, H. S. Loka, A. Othonos, and P. W. E. Smith, Appl. Phys. Lett. **68**, 2544 (1996).
[19] S. S. Prabhu, S. E. Ralph, M. R. Melloch, and E. S. Harmon, Appl. Phys. Lett. **70**, 2419 (1997).
[20] Q. Wu, M. Litz, and X.-C. Zhang, Appl. Phys. Lett. **68**, 2924 (1996).
[21] R. W. Ziolkowski and J. B. Judkins, J. Opt. Soc. Am. A **9**, 2021 (1992).
[22] P. Kužel, M. A. Khazan, and J. Kroupa, J. Opt. Soc. Am. B **16**, 1795 (1999).
[23] H. G. Roskos, M. C. Nuss, J. Shah, K. Leo, D. A. B. Miller, A. M. Fox, S. Schmitt-Rink, and K. Köhler, Phys. Rev. Lett. **68**, 2216 (1992).
[24] C. Waschke, H. G. Roskos, R. Schwedler, K. Leo, H. Kurz, and K. Köhler, Phys. Rev. Lett. **70**, 3319 (1993).
[25] H. J. Bakker, G. C. Cho, H. Kurz, Q. Wu, and X.-C. Zhang, J. Opt. Soc. Am. B **15**, 1795 (1998).
[26] G. Gallot and D. Grischkowsky, J. Opt. Soc. Am. B **16**, 1204 (1999).
[27] P. U. Jepsen, R. H. Jacobsen, and R. H. Keiding, J. Opt. Soc. Am. B **13**, 2424 (1996).
[28] S. M. Sze, *Semiconductor Devices* (Wiley, New York, 1985), p. 33.
[29] M. Stellmacher, J.-P. Schnell, D. Adam, and J. Nagle, Appl. Phys. Lett. **74**, 1239 (1999).
[30] D. H. Auston, *Ultrafast Optoelectronics, in Ultrashort Laser Pulses—Generation and Applications*, edited by W. Kaiser, Topics in Applied Physics Vol. 60 (Springer, Berlin, 1993), p. 183.
[31] C. Erginsoy, Phys. Rev. **79**, 1013 (1950).
[32] S. Wang, *Fundamentals of Semiconductor Theory and Device Physics* (Prentice–Hall, Englewood Cliffs, NJ, 1989).

Downloaded 24 Oct 2001 to 195.113.33.31. Redistribution subject to AIP license or copyright, see http://ojps.aip.org/japo/japcr.jsp